



OPEN Microstructures at the distal tip of ant chemosensory sensilla

Hannah R. Gellert¹, Daphné C. Halley², Zackary J. Sieb³, Jody C. Smith⁴ & Gregory M. Pask^{1,3,5}✉

Ants and other eusocial insects emit and receive chemical signals to communicate important information within the colony. In ants, nestmate recognition, task allocation, and reproductive distribution of labor are largely mediated through the detection of cuticular hydrocarbons (CHCs) that cover the exoskeleton. With their large size and limited volatility, these CHCs are believed to be primarily detected through direct contact with the antennae during behavioral interactions. Here we first use scanning electron microscopy to investigate the unique morphological features of CHC-sensitive basiconic sensilla of two ant species, the black carpenter ant *Camponotus pennsylvanicus* and the Indian jumping ant *Harpegnathos saltator*. These basiconic sensilla possess an abundance of small pores typical of most insect olfactory sensilla, but also have a large concave depression at the terminal end. Basiconic sensilla are enriched at the distal segments of the antennae in both species, which aligns with their proposed role in contact chemosensation of CHCs. A survey of these sensilla across additional ant species shows varied microstructures at their tips, but each possess surface textures that would also increase sensory surface area. These unique ant chemosensory sensilla represent yet another example of how specialized structures have evolved to serve the functional requirements of eusocial communication.

Reliable communication among individuals is of the utmost importance in successful animal societies. In eusocial insects like ants, bees, and wasps of Hymenoptera, this communication can employ several sensory modalities and drive a wide range of colony behaviors, as well as maintain the division of labor among different castes. The popular waggle dance of the honeybee recruits foraging workers within the hive using auditory, vibrational, chemical, and tactile signals¹. Ants rely heavily on chemical communication to signal foraging trails, detect invading non-nestmates, and maintain the reproductive hierarchy². Chemical or genetic manipulation of these chemosensory communication systems can trigger nestmate aggression, disrupt colony social behaviors, and even decrease reproductive success^{3–6}. Although solitary insects use chemical signals for social interactions between conspecifics like mating, it is widely believed that the necessary information used for higher forms of sociality required the diversification of chemical messages.

In terrestrial insects cuticular hydrocarbons (CHCs) provide a hydrophobic barrier that aids in water-retention, but CHCs have been co-opted by the eusocial insects to also serve as social cues^{7,8}. A structurally diverse range of CHCs in ants, bees, wasps, and termites have been implicated in nestmate recognition, reproductive division of labor, and task distribution^{9–16}. For example, a queen ant has a specific CHC profile that reflects her colony identity and reproductive status, with a matching CHC profile on her eggs that can distinguish them from those of workers¹⁷. The majority of CHCs identified on ants tend to have chain lengths of 25–35 carbons with varying levels of unsaturation and methyl branching¹⁸. At these sizes, ant CHCs are believed to have substantially low volatility and likely function in close- or near-contact interactions¹⁹.

Antennal detection of CHCs is mediated by specialized sensory hairs, or sensilla, that has been confirmed by electrophysiology in several ant species^{11,20–22}. Specifically, large basiconic sensilla are sensitive to a wide range of CHCs and house greater than 100 olfactory receptor neurons (ORNs)²³. The genes expressed in these ORNs are likely from the odorant receptor (OR) family, as heterologous expression studies have characterized ant ORs as highly specific CHC detectors^{24,25}. In these functional studies, the volatility of CHCs is augmented by either gas chromatography or direct application of heat^{21,22,24,25}. However, it is still unclear if CHC profiles are reliably detected by the antennae as volatile cues or if physical contact is necessary.

¹Department of Biology, Middlebury College, Middlebury, VT 05753, USA. ²Program in Environmental Studies, Middlebury College, Middlebury, VT 05753, USA. ³Program in Neuroscience, Middlebury College, Middlebury, VT 05753, USA. ⁴Sciences Technical Support Services, Middlebury College, Middlebury, VT 05753, USA. ⁵Program in Molecular Biology and Biochemistry, Middlebury College, Middlebury, VT 05753, USA. ✉email: gpask@middlebury.edu

Here, we use scanning electron microscopy (SEM) with the antennae of two distantly related ant species to provide insight into how morphology may facilitate antennal discrimination of CHC cues. The black carpenter ant, *Camponotus pennsylvanicus*, is common in eastern North America and colonies consist of morphologically distinct castes and an established reproductive. The Indian jumping ant, *Harpegnathos saltator*, is much less complex with a single morphological worker caste. However, *H. saltator* colonies display reproductive plasticity where workers can transition to a reproductive pseudoqueen with a senescing or deceased queen. Despite their different social structures, we identify conserved structural features that may play a role in effective social communication.

Results and discussion

SEM analysis revealed that the basiconic sensilla of *C. pennsylvanicus* feature a large concave depression surrounded by several smaller pores at the distal end of the sensillum (Fig. 1a,c,e,g). In *C. pennsylvanicus* minor workers, the small multiporous openings have a mean diameter of $0.07 \mu\text{m} \pm 0.009 \mu\text{m}$ ($n = 5$); meanwhile, the terminal depression is approximately $1.4 \mu\text{m} \pm 0.11 \mu\text{m}$ in width and $0.39 \mu\text{m} \pm 0.014 \mu\text{m}$ in height ($n = 5$). This sensillar microstructure was conserved in various female morphs of *C. pennsylvanicus*: nanitics (smaller first workers), minors, intermediates, majors, and queens (data not shown). Furthermore, basiconic sensilla on the antennae of the ponerine ant, *H. saltator*, also possessed a concave depression at the tip (Fig. 1b,d,f,h). In *H. saltator* workers, the small multiporous openings are $0.09 \mu\text{m} \pm 0.013 \mu\text{m}$ in diameter ($n = 5$); meanwhile, the terminal depression is approximately $1.4 \mu\text{m} \pm 0.11 \mu\text{m}$ in width and $0.39 \mu\text{m} \pm 0.06 \mu\text{m}$ in height ($n = 5$). To ensure that our observations were not due to dehydration effects of our solvent washes, samples were prepped without hexanes or any washes and still displayed similar microstructures (Supplementary Fig. S1).

From SEM imaging it is unclear whether the visible depression at the end of the basiconic sensilla in *C. pennsylvanicus* and *H. saltator* is merely a concave tip or a terminal pore that connects directly to the sensillar lymph. A concave depression would increase surface area for more efficient contact with surfaces (nestmate cuticle or others) during antennation. A terminal pore would be similar to uniporous gustatory sensilla found in insect taste appendages, where tastants enter the lymph through contact with a single large opening at the tip of the sensillum²⁶. CHCs contacted by basiconic sensilla during antennation could traverse this terminal pore, enter the sensillum lymph where it is solubilized by a family of odorant-binding and chemosensory proteins, and interact with the ORNs²⁷. Functionally assessing the individual contribution of a possible terminal pore presents a significant experimental challenge as a delivered stimulus could enter the sensillum lymph through the many smaller pores as well. Further imaging with transmission electron microscopy (TEM) could investigate this question of basiconic sensillum tip ultrastructure and potential lymph continuity.

Our structural observations of ant basiconic sensilla seem to align with previous functional and neuroanatomical studies that have characterized these sensilla as detectors of CHCs and general odorants^{11,20–23}. Electrophysiological recordings from several ant species have found that ORNs within basiconic sensilla respond to a wide range of linear and methyl-branched hydrocarbons, including many that are found in ant cuticular extracts. Basiconic ORNs are also sensitive to general odorants, such as alcohols, esters, and acids, that are relatively smaller and more volatile than CHCs^{21,22}. It is worth noting that ant basiconic sensilla are innervated by ~100 ORNs^{23,28}. A sensillum housing so many ORNs that respond to diverse chemical stimuli perhaps benefits from specialized structural features that can enable the efficient detection of both volatile and contact-mediated cues.

We then imaged full-length antennae of both *C. pennsylvanicus* and *H. saltator* to quantify the abundance of basiconic sensilla on each segment (Fig. 2). In all five female *C. pennsylvanicus* castes and *H. saltator* workers, basiconic sensilla were significantly enriched in the distal segments and accounted for >68% of total variation (Fig. 2, Table 1, two-way ANOVA, $p < 0.0001$ for all datasets). Interestingly, a significant bias toward ventral position of these sensilla was found in *C. pennsylvanicus* minor and major workers, but no other samples (Supplementary Fig. S2, two-way ANOVA, $p = 0.0034$ for minors and $p < 0.0001$ for majors). At the extremes of the funiculus, the 10th segments of *C. pennsylvanicus* minors and *H. saltator* workers had 47.3 ± 4.8 and 63.8 ± 3.7 basiconic sensilla, respectively, and decreased proximally along the antenna until the pedicel, where no basiconic sensilla were present across both species and all castes of *C. pennsylvanicus*. Increased basiconic sensilla presence at the distal end and/or ventral surface of an antennae coincides with the regions that predominantly contact other ants during typical social interactions, providing further support for a model of contact- or near contact-mediated recognition of CHCs²⁹.

We expanded our characterization of these unique basiconic sensillar microstructures to other subfamilies of ants. Notably, basiconic sensilla in *Formica exsectoides* (subfamily Formicinae) and *Pogonomyrmex occidentalis* (subfamily Myrmicinae) possessed similar concave depressions at their tips along with numerous smaller pores (Fig. 3a,b), similar to what was found in *C. pennsylvanicus* (also subfamily Formicinae) and *H. saltator* (subfamily Ponerinae). However, in *Atta cephalotes* (subfamily Myrmicinae), *Linepithema humile* (subfamily Dolichoderinae), *Tapinoma sessile* (subfamily Dolichoderinae), and *O. biroi* (subfamily Dorylinae) no noticeable depression was observed at the tip of basiconic sensilla (Fig. 3c–f, see Supplementary Fig. S3 for subfamily relationships). Instead, the sensilla displayed rounded and multiporous ends with some possessing elaborate furrows along the distal surface. These furrows on the surface of olfactory sensilla have been observed in several insects and have been theorized to function as canals in directing hydrophobic odorants into pores^{30,31}. It is possible that the sensillar furrows represent another morphological strategy to increase sensory surface area and retain CHCs. Although there is no clear evolutionary pattern on the presence of terminal depressions of basiconic sensilla (Supplementary Fig. S3), further imaging across the Formicidae subfamilies may reveal a social, chemical, or morphological role.

Ant antennae across many species have been imaged by SEM before, yet these specific features of basiconic sensilla have not been previously described^{22,23,29,32,33}. Examination of previous images shows faint indications of

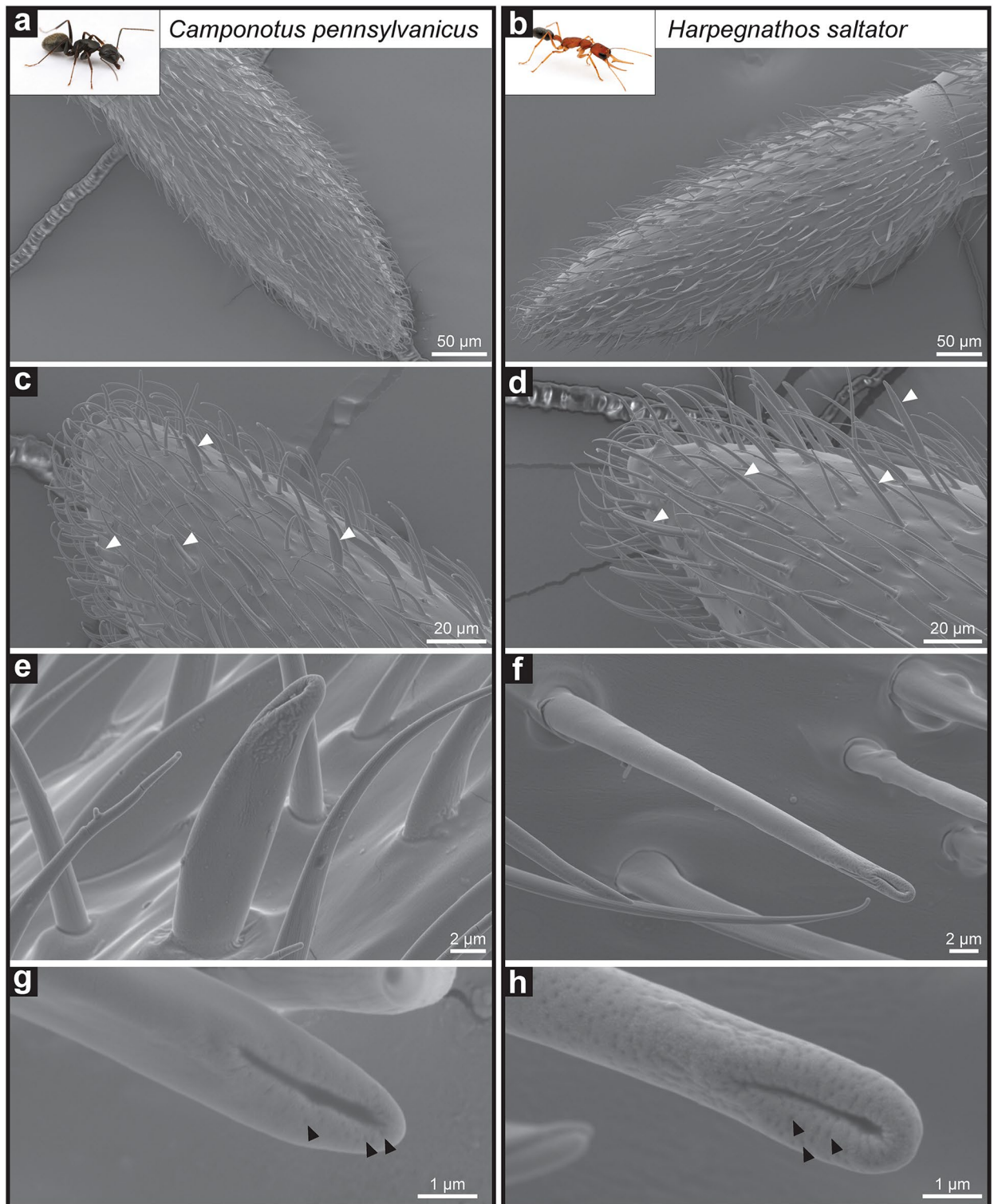


Figure 1. Morphology of chemosensory sensillum in *C. pennsylvanicus* and *H. saltator*. Representative images of a *Camponotus pennsylvanicus* minor worker (a,c,e,g) and *Harpegnathos saltator* worker (b,d,f,h). Panels depict the full 10th segment of the funiculus (a,b) and its distal tip with some basiconic sensilla highlighted by white arrowheads (c,d). Images of a basiconic single sensillum (e,f) and the terminal end (g,h) depict a large concave depression and several smaller pores indicated by black arrowheads. Inset ant images are provided courtesy of Alex Wild (alexanderwild.com).

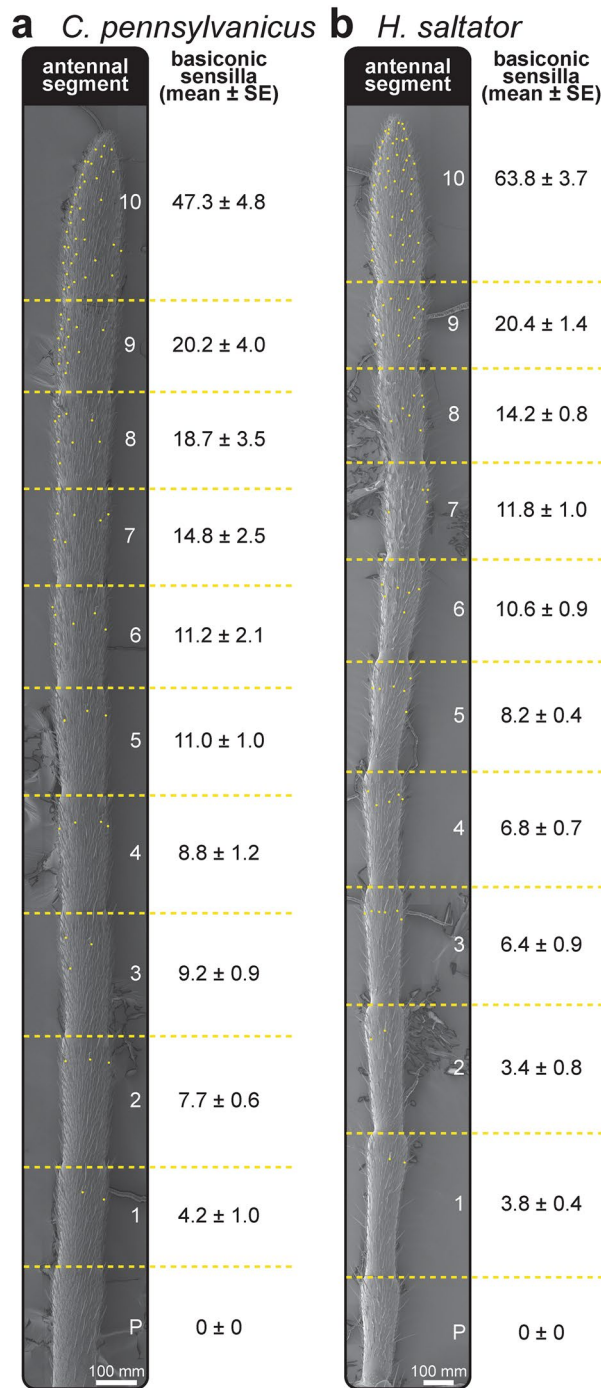


Figure 2. Distal abundance of basiconic sensilla across two distantly related ant species. Images of the funiculus segments (1–10) and pedicel (P) (left) and basiconic sensilla counts (right) of a *C. pennsylvanicus* minor worker (a) and *H. saltator* worker (b). Yellow dots denote the position and overall distribution of basiconic sensilla. Sensillum counts represent the average and standard error of the dorsal and ventral total per individual ($n = 5-6$).

the terminal concave depression, but higher accelerating voltages of 15–20 kV result in deeper tissue penetration by the electrons, thus potentially causing a loss of surficial features^{22,23}. In our case, reduction of the accelerating voltage to 5 kV revealed clear depressions and provided increased resolution of the smaller olfactory pores. Of note is a recent paper that used a reduced accelerating voltage to image intact and living *C. japonicus* ant antennae, and a terminal depression at the tip of a basiconic sensillum was clearly visible²³. As advances in electron optics continue, lower accelerating voltages may increase the surficial resolving power of insect SEM imaging.

Caste	Antennal segment										
	P	1	2	3	4	5	6	7	8	9	10
<i>Nanitic</i>	0.0 ± 0.0	3.3 ± 0.6	3.8 ± 1.2	5.5 ± 1.3	6.2 ± 1.0	7.5 ± 1.1	8.0 ± 1.7	9.5 ± 2.6	10.2 ± 2.8	11.0 ± 3.5	37.0 ± 6.2
<i>Minor</i>	0.0 ± 0.0	4.2 ± 1.0	7.7 ± 0.6	9.2 ± 0.9	8.8 ± 1.2	11.0 ± 1.0	11.2 ± 2.1	14.8 ± 2.5	18.7 ± 3.5	20.2 ± 4.0	47.3 ± 4.8
<i>Intermediate</i>	0.0 ± 0.0	4.2 ± 0.4	6.6 ± 0.4	8.0 ± 0.7	9.0 ± 1.2	10.0 ± 1.0	12.0 ± 0.5	14.8 ± 1.2	17.6 ± 1.2	17.6 ± 1.2	50.0 ± 2.9
<i>Major</i>	0.0 ± 0.0	3.8 ± 0.9	6.6 ± 0.9	9.6 ± 0.5	9.8 ± 0.4	13.2 ± 0.9	14.2 ± 1.7	19.4 ± 2.4	21.6 ± 2.6	24.8 ± 4.6	61.2 ± 7.6
<i>Queen</i>	0.0 ± 0.0	2.4 ± 0.4	6.4 ± 0.5	8.0 ± 1.1	9.0 ± 1.4	11.8 ± 0.7	14.8 ± 0.7	16.2 ± 1.4	22.4 ± 1.2	25.0 ± 1.6	64.8 ± 2.6

Table 1. Antennal distribution of basiconic sensilla across different *C. pennsylvanicus* castes. Sensillum counts represent the average and standard error of the dorsal and ventral total for each antennal segment ($n = 5-6$).

As a major sensory interface for insects, the varied structural aspects of cuticular features serve specific roles in sensory function. For example, the long thin hairs of plumose mosquito antennae are firmly coupled to the antennal shaft and can efficiently transmit the wingbeat frequencies of conspecifics through the shaft to the Johnston's organ³⁴. Our morphological characterization of a specialized chemosensory sensillum in ants identifies features that align with known functional and behavioral aspects of CHC detection and nestmate recognition, with both the increased surface area of the terminal microstructure and the distal abundance of ant basiconic sensilla supporting contact recognition of CHCs. Although it has been shown that close-range recognition of non-nestmate CHCs can occur without antennal contact¹⁹, recognition behaviors of free-moving ants begin with investigative antennation with repeated contact before a decision is made regarding acceptance or aggression³⁵⁻³⁷. Our findings support the further investigation of questions in non-model insects, as the identification of unique morphological structures can inform and support our understanding of well-documented behaviors.

Methods

Animals. All female castes of *Camponotus pennsylvanicus* and workers of *Formica exsectoides* were collected locally in Vermont. *Harpegnathos saltator* were obtained from an in-house laboratory colony. *Pogonomyrmex occidentalis* workers were purchased from TruBlu Supply. Workers from the following species were generously donated by the following individuals: *Atta cephalotes* (M. Gilbert, University of Pennsylvania), *Linepithema humile* (L. Martins and N. Tsutsui, University of California, Berkeley) *Tapinoma sessile* (G. Buczkowski, Purdue University), and *Ooceraea biroii* (W. Tribble, Harvard University). Only female ants were imaged as male ants have already been shown to not possess basiconic sensilla^{23,38}.

Scanning electron microscopy (SEM). *Specimen preparation.* For each insect anesthetized by CO₂, the head was removed with antennae intact. The head and both antennae were sequentially washed in a watch glass with pure hexanes, pure acetone, and 95% ethanol, with each solvent applied only after the previous had fully evaporated. Variations in specimen preparation were also performed and detailed in Supplementary Fig. S1. The left antenna was mounted on a ½" slotted head aluminum specimen mount, dorsal side up, then removed from the head. On the same mount, the right antenna was positioned ventral side up, then removed from the head. Samples were coated in gold-palladium using an Ernest Fullam Inc. EffaCoater Au-Pd Sputter Coater.

Imaging and analysis. Images were acquired using a Tescan Vega 3 LMU Scanning Electron Microscope with an accelerating voltage of 5 kV and beam intensity of 6. High-quality imaging of whole antennae was performed with automated scanning and post-hoc montage stitching using Tescan VegaTC software image snapper wizard.

Images were analyzed for the presence of basiconic sensilla along the antenna. Basiconic sensilla were defined as blunt-tipped sensory hairs with a circular socket at the base. For *C. pennsylvanicus* and *H. saltator*, imaging and counting of basiconic sensilla included the funiculus and pedicel. The scape was excluded after no basiconic sensilla could be found. Each segment of the antenna was numbered, with segment three being the proximal segment and segment thirteen being the distal segment at the tip of the antenna. Basiconic sensilla were counted only if the base of the sensillum was visible to prevent possible double counting of sensilla from the opposite side. This process was repeated for the dorsal and ventral sides, and then combined for an estimate of the total basiconic sensilla present on a single antenna.

Statistical analysis of basiconic sensilla counts was performed using Prism 9 (Graphpad). Two-way ANOVA tests were used to determine the effects of antennal segment and dorsal/ventral surface on sensillum abundance, with Bonferroni's multiple comparisons tests for post-hoc comparisons between dorsal/ventral abundance at each segment.

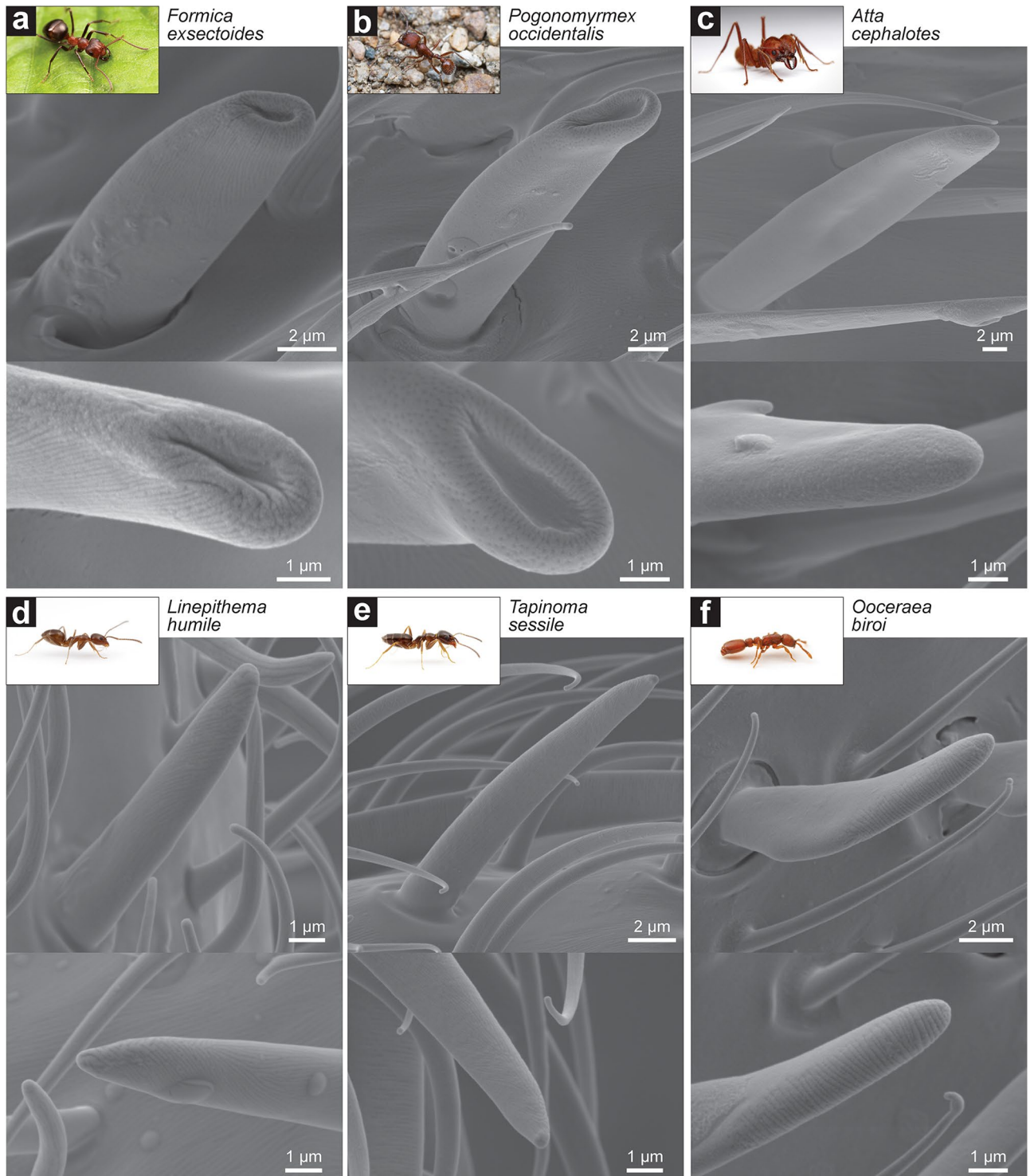


Figure 3. Basiconic sensillum morphology across major subfamilies of ants. Images of both the basiconic sensillum (top) and its tip (bottom) of (a) *Formica exsectoides* worker (subfamily Formicinae), (b) *Pogonomyrmex occidentalis* worker (subfamily Myrmicinae), (c) *Atta cephalotes* super major (subfamily Myrmicinae), (d) *Linepithema humile* worker (subfamily Dolichoderinae), (e) *Tapinoma sessile* worker (subfamily Dolichoderinae), and (f) *Ooceraea biroi* (subfamily Dorylinae). Inset ant images are provided courtesy of Alex Wild (alexanderwild.com).

Data availability

Imaging data and analyses are available from the corresponding author upon request.

Received: 6 June 2022; Accepted: 28 September 2022

Published online: 11 November 2022

References

- Thom, C., Gilley, D. C., Hooper, J. & Esch, H. E. The scent of the waggle dance. *PLoS Biol.* **5**, e228 (2007).
- Hölldobler, B. & Wilson, E. O. *The Ants* (Harvard University Press, 1990). https://doi.org/10.1007/978-3-662-10306-7_7.
- Torres, C. W., Brandt, M. & Tsutsui, N. D. The role of cuticular hydrocarbons as chemical cues for nestmate recognition in the invasive Argentine ant (*Linepithema humile*). *Insect Soc.* **54**, 363–373 (2007).
- Yan, H. *et al.* An engineered orco mutation produces aberrant social behavior and defective neural development in ants. *Cell* **170**, 736–747.e9 (2017).
- Tribble, W. *et al.* Orco mutagenesis causes loss of antennal lobe glomeruli and impaired social behavior in ants. *Cell* **170**, 727–735.e10 (2017).
- Ferguson, S. T., Park, K. Y., Ruff, A. A., Bakis, I. & Zwiebel, L. J. Odor coding of nestmate recognition in the eusocial ant *Camponotus floridanus*. *J. Exp. Biol.* **223**, 215400 (2020).
- Blomquist, G. J. & Ginzl, M. D. Chemical ecology, biochemistry, and molecular biology of insect hydrocarbons. *Annu. Rev. Entomol.* **66**, 45–60 (2021).
- Yan, H. & Liebig, J. Genetic basis of chemical communication in eusocial insects. *Gene Dev.* **35**, 470–482 (2021).
- Wagner, D., Tissot, M., Cuevas, W. & Gordon, D. M. Harvester ants utilize cuticular hydrocarbons in nestmate recognition. *J. Chem. Ecol.* **26**, 2245–2257 (2000).
- Wagner, D. *et al.* Task-related differences in the cuticular hydrocarbon composition of harvester ants *Pogonomyrmex barbatus*. *J. Chem. Ecol.* **24**, 2021–2037 (1998).
- Holman, L., Jørgensen, C. G., Nielsen, J. & d’Ettorre, P. Identification of an ant queen pheromone regulating worker sterility. *Proc. R. Soc. B Biol. Sci.* **277**, 3793–3800 (2010).
- Oystaeyen, A. V. *et al.* Conserved class of queen pheromones stops social insect workers from reproducing. *Science* **343**, 287–290 (2014).
- Liebig, J., Peeters, C., Oldham, N. J., Markstädter, C. & Hölldobler, B. Are variations in cuticular hydrocarbons of queens and workers a reliable signal of fertility in the ant *Harpegnathos saltator*?. *Proc. Natl. Acad. Sci.* **97**, 4124–4131 (2000).
- Liebig, J., Eliyahu, D. & Brent, C. S. Cuticular hydrocarbon profiles indicate reproductive status in the termite *Zootermopsis nevadensis*. *Behav. Ecol. Sociobiol.* **63**, 1799–1807 (2009).
- van Zweden, J. S., Dreier, S. & d’Ettorre, P. Disentangling environmental and heritable nestmate recognition cues in a carpenter ant. *J. Insect Physiol.* **55**, 159–164 (2009).
- Greene, M. J. & Gordon, D. M. Cuticular hydrocarbons inform task decisions. *Nature* **423**, 32–32 (2003).
- Endler, A., Liebig, J. & Hölldobler, B. Queen fertility, egg marking and colony size in the ant *Camponotus floridanus*. *Behav. Ecol. Sociobiol.* **59**, 490–499 (2006).
- Martin, S. & Drijfhout, F. A review of ant cuticular hydrocarbons. *J. Chem. Ecol.* **35**, 1151 (2009).
- Brandstaetter, A. S., Endler, A. & Kleineidam, C. J. Nestmate recognition in ants is possible without tactile interaction. *Naturwissenschaften* **95**, 601–608 (2008).
- D’Ettorre, P., Heinze, J., Schulz, C., Francke, W. & Ayasse, M. Does she smell like a queen? Chemoreception of a cuticular hydrocarbon signal in the ant *Pachycondyla inversa*. *J. Exp. Biol.* **207**, 1085–1091 (2004).
- Sharma, K. R. *et al.* Cuticular hydrocarbon pheromones for social behavior and their coding in the ant antenna. *Cell Rep.* **12**, 1261–1271 (2015).
- Ghaninia, M. *et al.* Chemosensory sensitivity reflects reproductive status in the ant *Harpegnathos saltator*. *Sci. Rep. UK 7*, 3732 (2017).
- Nakanishi, A., Nishino, H., Watanabe, H., Yokohari, F. & Nishikawa, M. Sex-specific antennal sensory system in the ant *Camponotus japonicus*: Structure and distribution of sensilla on the flagellum. *Cell Tissue Res.* **338**, 79–97 (2009).
- Pask, G. M. *et al.* Specialized odorant receptors in social insects that detect cuticular hydrocarbon cues and candidate pheromones. *Nat. Commun.* **8**, 297 (2017).
- Slone, J. D. *et al.* Functional characterization of odorant receptors in the ponerine ant, *Harpegnathos saltator*. *Proc. Natl. Acad. Sci.* **114**, 8586–8591 (2017).
- Yosano, S. *et al.* Taste recognition through tarsal gustatory sensilla potentially important for host selection in leaf beetles (Coleoptera: Chrysomelidae). *Sci. Rep. UK 10*, 4931 (2020).
- McKenzie, S. K., Oxley, P. R. & Kronauer, D. J. Comparative genomics and transcriptomics in ants provide new insights into the evolution and function of odorant binding and chemosensory proteins. *BMC Genom.* **15**, 718 (2014).
- Takeichi, Y. *et al.* Putative neural network within an olfactory sensory unit for nestmate and non-nestmate discrimination in the Japanese carpenter ant: The ultra-structures and mathematical simulation. *Front. Cell. Neurosci.* **12**, 310 (2018).
- McKenzie, S. K., Fetter-Pruneda, I., Ruta, V. & Kronauer, D. J. C. Transcriptomics and neuroanatomy of the clonal raider ant implicate an expanded clade of odorant receptors in chemical communication. *Proc. Natl. Acad. Sci.* **113**, 14091–14096 (2016).
- Riesgo-Escovar, J. R., Piekos, W. B. & Carlson, J. R. The *Drosophila* antenna: Ultrastructural and physiological studies in wild-type and lozenge mutants. *J. Comp. Physiol.* **180**, 151–160 (1997).
- Jeong, S. A., Kim, J., Byun, B.-K., Oh, H.-W. & Park, K. C. Morphological and ultrastructural characterization of olfactory sensilla in *Drosophila suzukii*: Scanning and transmission electron microscopy. *J. Asia Pac. Entomol.* **23**, 1165–1180 (2020).
- Ozaki, M. *et al.* Ant nestmate and non-nestmate discrimination by a chemosensory sensillum. *Science (New York, N Y)* **309**, 311–314 (2005).
- Mizutani, H. *et al.* Antenna cleaning is essential for precise behavioral response to alarm pheromone and nestmate–non-nestmate discrimination in Japanese carpenter ants (*Camponotus japonicus*). *Insects* **12**, 773 (2021).
- Göpfert, M. C., Briegel, H. & Robert, D. Mosquito hearing: Sound-induced antennal vibrations in male and female *Aedes aegypti*. *J. Exp. Biol.* **202**, 2727–2738 (1999).
- Carlin, N. F. & Hölldobler, B. The kin recognition system of carpenter ants (*Camponotus* spp.). *Behav. Ecol. Sociobiol.* **19**, 123–134 (1986).
- Carlin, N. F. & Hölldobler, B. The kin recognition system of carpenter ants (*Camponotus* spp.). *Behav. Ecol. Sociobiol.* **20**, 209–217 (1987).
- Rao, A. & Vinson, S. B. The initial behavioral sequences and strategies of various ant species during individual interactions with *Solenopsis invicta*. *Ann. Entomol. Soc. Am.* **102**, 702–712 (2009).
- Ghaninia, M. *et al.* Antennal olfactory physiology and behavior of males of the ponerine ant *Harpegnathos saltator*. *J. Chem. Ecol.* **44**, 999–1007 (2018).

Acknowledgements

We would like to thank Michael Gilbert, Lourenço Martins, Neil Tsutsui, Grzegorz Buczkowski, W. Tribble, and Daniel Kronauer for providing ant specimens and Alex Wild for sharing all ant images inset in Figs. 1 and 3. We

also thank Stephen Ferguson, Sarah Lower, Jason Pitts, and Hua Yan for insightful comments on the manuscript. We also thank the George I. Allen Trust for funding the acquisition of the Tescan Vega 3 LMU Scanning Electron Microscope and the Middlebury Undergraduate Research Office and Biology Department for providing student research support.

Author contributions

H.R.G., D.C.H., and G.M.P. designed the experiments. H.R.G., D.C.H., and Z.J.S. prepared and imaged antennal samples. H.R.G., D.C.H., Z.J.S., and J.C.S. optimized imaging conditions. H.R.G. and G.M.P. performed data analyses and prepared figures and tables. H.R.G. and G.M.P. wrote the manuscript and all authors reviewed the manuscript.

Competing interests

The authors declare no competing interests.

Additional information

Supplementary Information The online version contains supplementary material available at <https://doi.org/10.1038/s41598-022-21507-7>.

Correspondence and requests for materials should be addressed to G.M.P.

Reprints and permissions information is available at www.nature.com/reprints.

Publisher's note Springer Nature remains neutral with regard to jurisdictional claims in published maps and institutional affiliations.



Open Access This article is licensed under a Creative Commons Attribution 4.0 International License, which permits use, sharing, adaptation, distribution and reproduction in any medium or format, as long as you give appropriate credit to the original author(s) and the source, provide a link to the Creative Commons licence, and indicate if changes were made. The images or other third party material in this article are included in the article's Creative Commons licence, unless indicated otherwise in a credit line to the material. If material is not included in the article's Creative Commons licence and your intended use is not permitted by statutory regulation or exceeds the permitted use, you will need to obtain permission directly from the copyright holder. To view a copy of this licence, visit <http://creativecommons.org/licenses/by/4.0/>.

© The Author(s) 2022